

Supporting Information

Sandwich-Structured PEO-Based Composite Solid-State Electrolyte for Lithium-Sulfur Batteries

Jingyi Wu^a, *Ruiqing Liu*^{a,*}, *Hui Cheng*^a, *Chenxu Tian*^a, *Yu Zhang*^a, *Xiaoyu Wang*^a,
Ying Liu^a, *Wenxiu Liu*^a, *Xiujing Lin*^a, *Cuie Zhao*^{a,*}, *Li Shi*^a, *Xiaomiao Feng*^{a,*},
Yanwen Ma^{a,*}

^a State Key Laboratory of Flexible Electronics (LoFE)

Institute of Advanced Materials (IAM)

School of Materials Science and Engineering

Nanjing University of Posts & Telecommunications

9 Wenyuan Road, Nanjing 210023, China.

E-mail: iamrqliu@njupt.edu.cn; iamcezhao@njupt.edu.cn; iamxmfeng@njupt.edu.cn;
iamywma@njupt.edu.cn;

Experimental Section

Preparation of PEO-TiO₂ composite solid-state electrolyte. The PEO powder, LiTFSI powder were stored in a glove box. Four washed small glass vials were taken and brought into the glove box and 200 mg of PEO, and 72.4 mg of LiTFSI powder were weighed into 4 mL of acetonitrile solvent. After stirring for 24 h, TiO₂ powders of different masses were added to the homogeneous solution. The homogeneous electrolyte solution was obtained after sufficient stirring for 24 h. Take the cellulose film with a diameter of 19 mm, place it on a PTFE plate, take an appropriate amount of solution cast on the cellulose film, and then turn it over and cast it on the other side after it is evenly dispersed, and pay attention to avoid air bubbles. Afterwards, the PTFE plate was placed in a glove box and left to stand for 48 h. The PEO-TiO₂ composite solid electrolytes with TiO₂ mass fractions of 0 wt%, 3 wt%, 5 wt%, 10 wt%, and 15 wt% were obtained, which were respectively noted as PEO-LiTFSI, CSE-3, CSE-5,

CSE-10, and CSE-15.

Preparation of sulfur cathode. 70 mg of sulfur powder and 30 mg of Cabot activated carbon were ground in an agate mortar for 30 min to make a homogeneous mixture. The mixture was spread evenly on the bottom of the magnetic boat, which was wrapped with tinfoil and pierced with small holes. The magnetic boat was placed in a tube furnace and heated up to 165°C with a heating rate of 1°C min⁻¹ and held for 12 h. The prepared material was an S@C composite. The S@C composite material, conductive carbon black, and PVDF with the mass ratio of 7:2:1, were ground in a mortar for 30 min. After mixing well, the material was poured into a small beaker, and an appropriate amount of NMP solution was added, and the homogeneous slurry was obtained by mixing for 8 h. The above uniform slurry was casted on the cleaned carbon-coated aluminum foil collector and coated with a thickness of 300 μm. After that, it was dried in a blast drying oven at 60°C for 30 min and then transferred to a vacuum drying oven at 60°C for 24 h. Finally, the resulting film was cut into 12 mm rounds. The sulfur loading of each positive electrode was about 1 mg cm⁻².

Assembly of all-solid-state lithium-sulfur batteries. The all-solid-state lithium-sulfur batteries were assembled in the order of cathode shell, cathode, electrolyte, anode, steel sheet, shrapnel, and anode shell. The all-solid-state lithium-sulfur batteries prepared with different electrolytes were named as Li//PEO-LiTFSI//S@C, Li//CSE-5//S@C, Li//CSE-10//S@C, and Li//CSE-15//S@C, respectively, and the above processes were completed in an argon-filled glove box (the content of both H₂O and O₂ was less than 0.1 ppm). The cells were left to stand for 4 h and then prepared for measurement.

Physical and chemical characterizations. The surface and cross-section morphologies of different electrolytes, as well as the morphology of lithium foils after cycling, were characterized by scanning electron microscopy (SEM, S-4800, Hitachi). X-ray diffraction (XRD) was carried out by a D8 Advance A25 X-ray powder diffractometer (BRUKER, Germany) with a measuring range of 10~80° and a scanning rate of 10° min⁻¹. The thermal stability of the solid electrolytes was investigated using a thermogravimetric analyzer (TGA STA-449F3 Netzsch) under a N₂ atmosphere, with a temperature range of 25~600°C, and a heating rate of 10°C min⁻¹. The thermal

behavior of different electrolyte membranes was analyzed using a differential scanning calorimeter (DSC-214 Polyma, Netzsch) with a N₂ atmosphere in the temperature range from -70 to 90°C and a heating rate of 10°C min⁻¹.

Electrochemical performance testing.

Electrochemical impedance spectroscopy (EIS) test: The cell was tested using an electrochemical workstation (CHI-660e) with a frequency range of 0.01~10⁶ Hz and an amplitude of 5 mV.

Cyclic voltammetry (CV) test: The cells were characterized using an electrochemical workstation (VMP3, Bio-logic) with a voltage range of 1.7~2.8 V and a sweep rate of 0.1~0.4 mV s⁻¹.

Electrochemical window test: The electrochemical stability of the electrolyte was evaluated by measuring its electrochemical stability window, which reflects its resistance to electrochemical corrosion at specific potentials. A semi-blocking cell was assembled by sandwiching the electrolyte between a lithium sheet (serving as both the counter and reference electrode) and a stainless steel sheet (acting as the working electrode). The electrochemical stability window was tested on a Bio-logic VMP3 electrochemical workstation using linear scanning voltammetry (LSV) with a scan rate of 0.5 mV s⁻¹ and a voltage range of 0~6 V.

Ionic conductivity test: Ionic conductivity is a critical parameter for evaluating polymer electrolytes, and the solid-state electrolyte should have excellent ionic conductivity to facilitate ion transport and good electronic insulation, thus effectively reducing self-discharge. To measure ionic conductivity, the electrolyte is sandwiched between two stainless steel sheets and using an electrochemical workstation with a temperature range of 30-70°C, a frequency range of 0.01-10⁶ Hz, and an amplitude of 5 mV. The ionic conductivity δ is calculated according to the following equation:

$$\delta = \frac{L}{R_b S} \quad (1-1)$$

Where δ is the ionic conductivity of the electrolyte membrane (S cm⁻¹); R_b is the body resistance of the electrolyte (Ω); L is the thickness of the electrolyte (cm); and S is the effective contact area between the electrolyte and the stainless steel sheet (cm²).

Lithium-ion transference number test: The lithium-ion transference number (t_{Li^+}) represents the proportion of the total current carried by lithium ions within the electrolyte. To enhance lithium-ion transport efficiency and prevent the migration of non-lithium ions and anions, polymer solid-state electrolytes must exhibit a high lithium-ion transference number. The impedance before and after polarization as well as the polarization current were tested at a constant voltage of 10 mV, and the lithium-ion transference number t_{Li^+} was calculated according to the following equation:

$$t_{Li^+} = \frac{I_s(\Delta V - I_0 R_0)}{I_0(\Delta V - I_s R_s)} \quad (1-2)$$

Where ΔV represents the polarization voltage (10 mV); I_0 and I_s represent the current values (μA) of the tested cell under the initial and steady-state currents, respectively; and R_0 and R_s are the corresponding interfacial charge transfer resistances (Ω) before and after polarization.

Calculate the lithium-ion diffusion coefficient (Randles-sevcik equation):

$$I_p = 2.69 \times 10^5 n^{1.5} A D_{Li^+}^{0.5} C_{Li} v^{0.5} \quad (1-3)$$

Herein, I_p , D_{Li^+} , n , A , C_{Li} , and v denote the peak current, lithium-ion diffusion coefficient, number of electrons transferred, effective electrode area, lithium-ion concentration in the electrolyte, and scan rate, respectively. The lithium-ion diffusion coefficient can be determined utilizing this equation.

Symmetric battery test: The cycling performance of lithium symmetric battery is characterized to assess the lithium stability of the solid-state electrolyte. The lithium deposition/ stripping experiments were performed at a current density of 0.1 mA cm⁻². The batteries were initially charged at constant current for 1 h, and then discharged at constant current for 1 h for a long cycle. Rate tests were performed using different current densities (0.02, 0.05, 0.1, 0.2, and 0.5 mA cm⁻²) with a charge/discharge time of 1 h, respectively, and 10 cycles were carried out at each current density.

Constant-current charge/discharge test: The constant-current charge/discharge test involves charging/discharging processes by applying a constant and continuous current under a specific voltage range. Key parameters, such as current, voltage, time,

charging/discharging specific capacity, rate performance, voltage plateau, Coulombic efficiency, capacity curves, etc, are recorded simultaneously. After assembling Li-S solid-state full batteries or lithium-symmetric batteries, the tests were conducted using the LAND Battery Test System (LAND CT2001A).

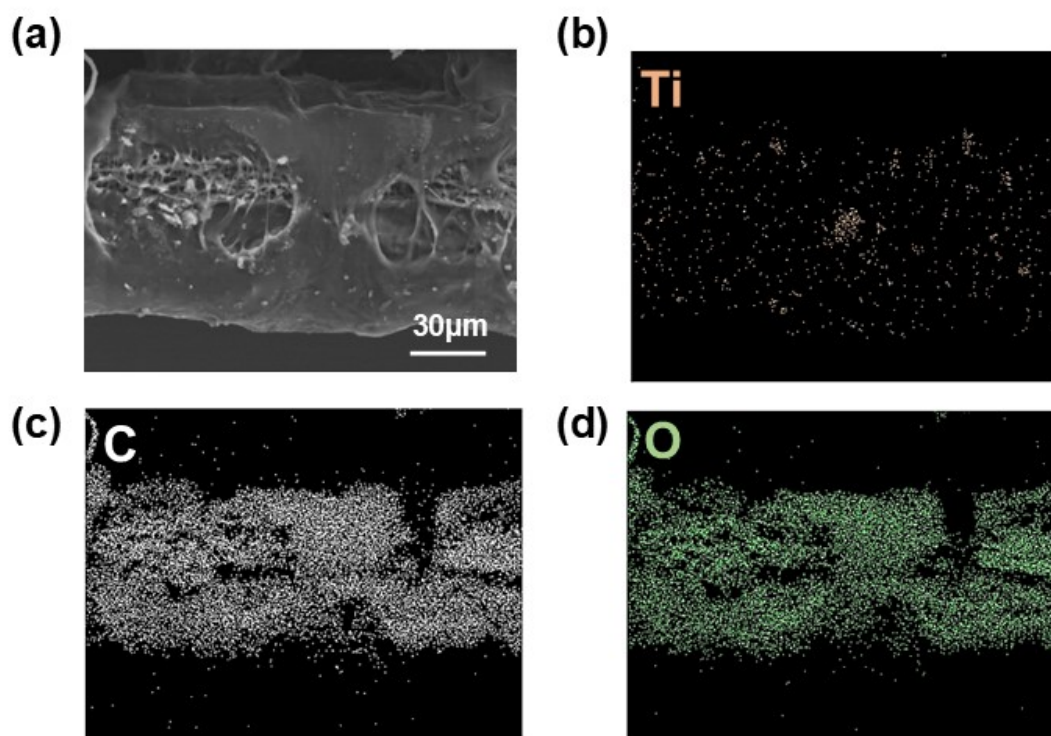


Figure S1. The elements mapping on the cross-section of the CSE-5 electrolyte.

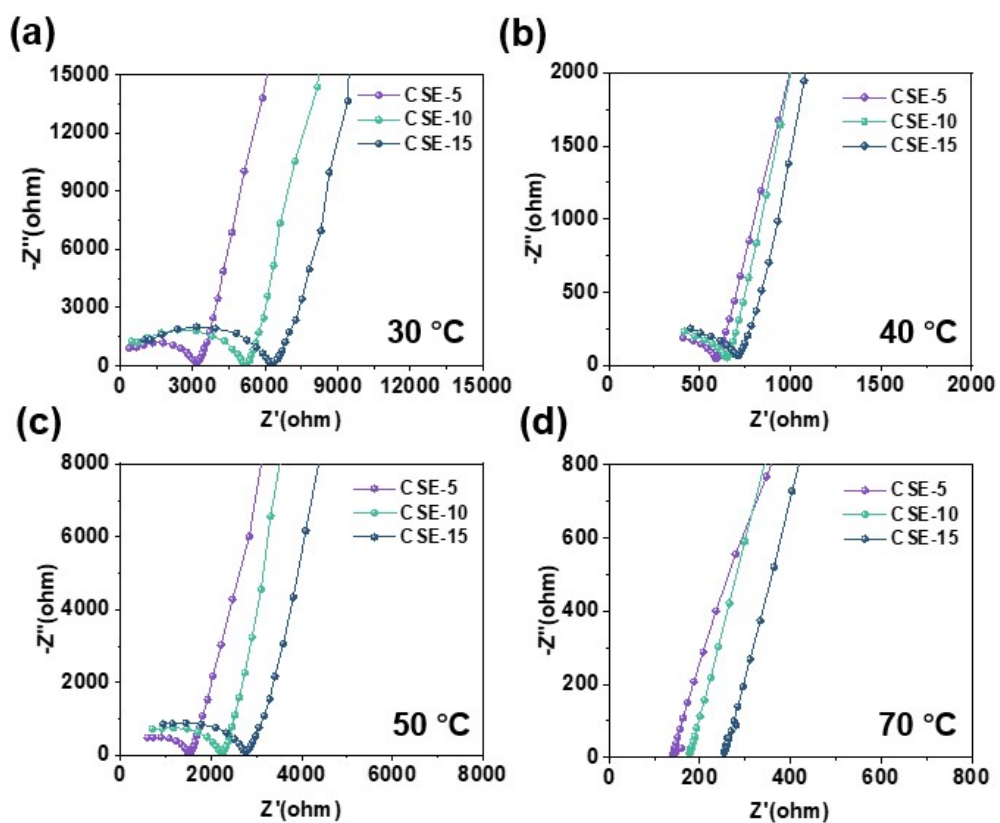


Figure S2. (a-d) Electrochemical impedance spectra (EIS) of CSE-5, CSE-10, and CSE-15 solid electrolyte membranes at different temperatures.

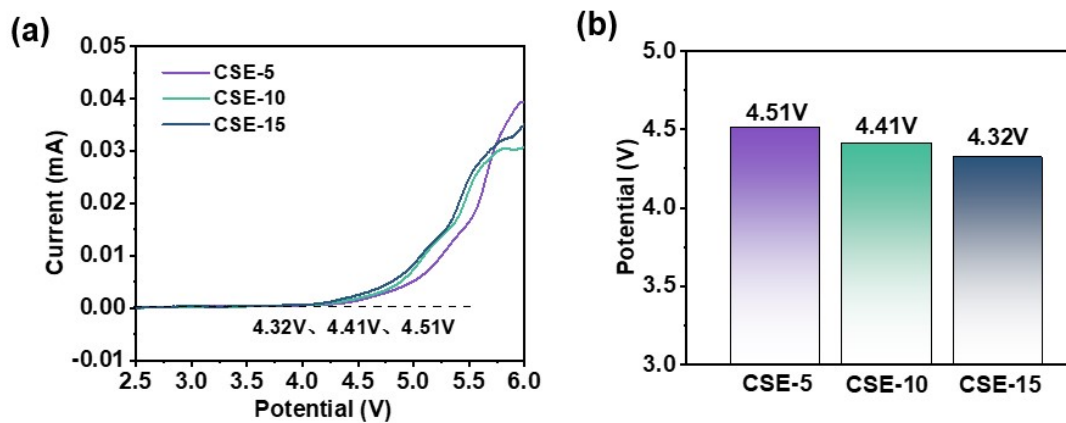


Figure S3. (a) Linear scanning voltammograms of three electrolytes, CSE-5, CSE-10, and CSE-15, at 40°C; (b) Summary plots of the decomposition voltages of the three electrolytes at 40°C.

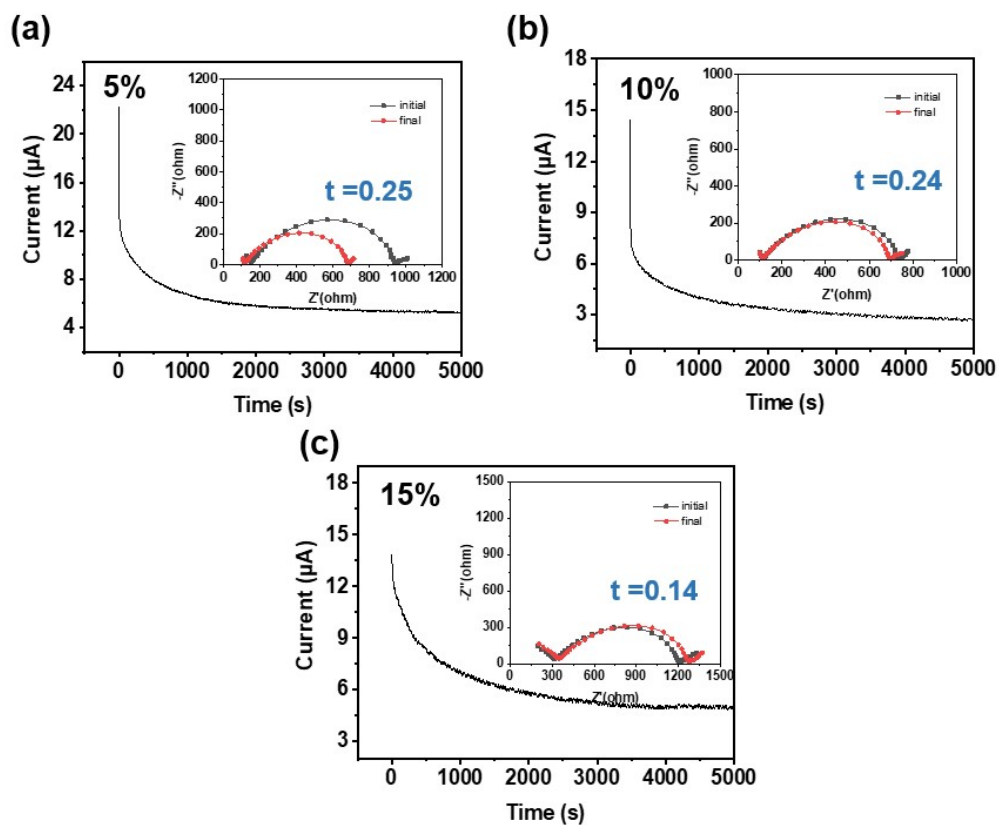


Figure S4. (a) Timing current curves and EIS of Li//CSE-5//Li cell; (b) Li//CSE-10//Li cell, (c) Li//CSE-15//Li cell measured at 40°C.

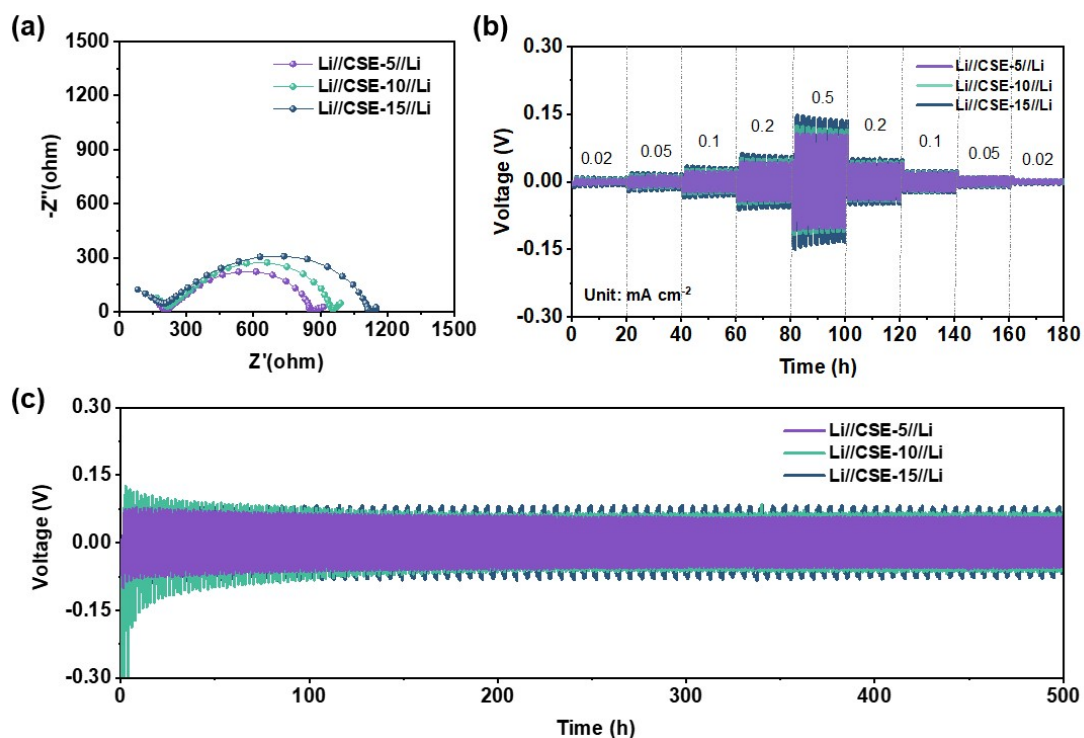


Figure S5. (a) EIS of Li//CSE-5//Li cell, Li//CSE-10//Li cell, Li//CSE-15//Li cell at 40°C; (b) Voltage-time profiles of Li//CSE-5//Li cell, Li//CSE-10//Li cell, Li//CSE-15//Li cell at 40°C at different current density; (c) voltage-time profiles of Li//CSE-5//Li, Li//CSE-10//Li, and Li//CSE-15//Li cells at 40°C with a current density of 0.1 mA cm⁻².

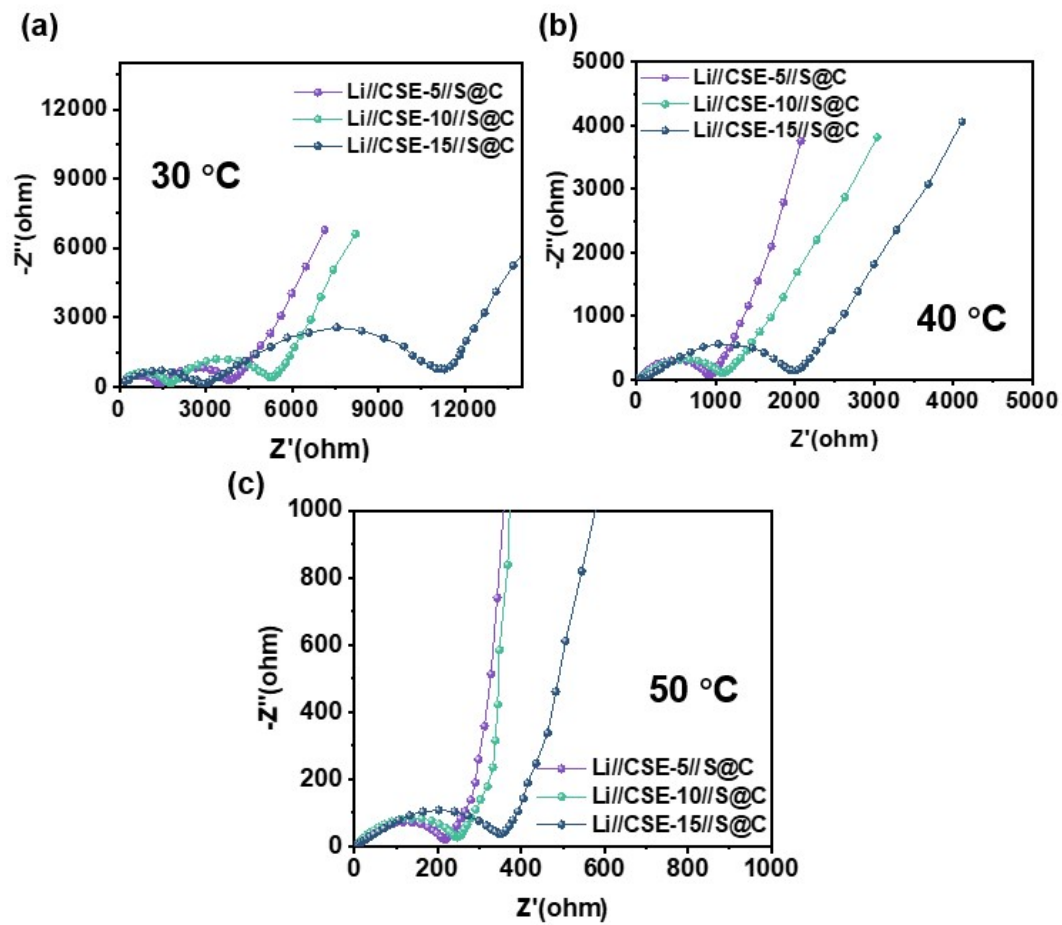


Figure S6. EIS of Li//CSE-5//S@C, Li//CSE-10//S@C, and Li//CSE-15//S@C solid-state batteries at (a) 30°C, (b) 40°C, and (c) 50°C.

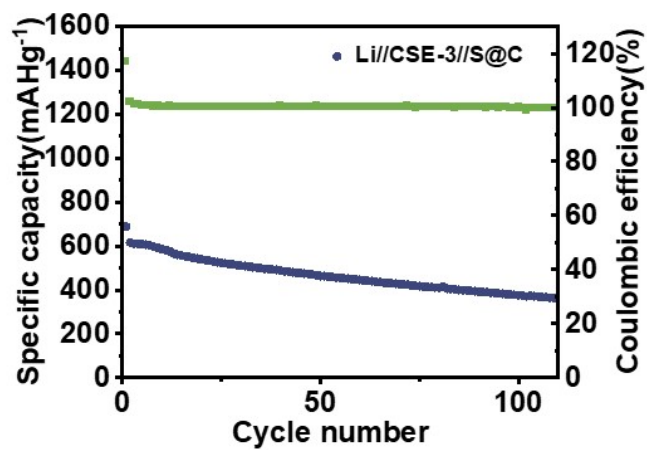


Figure S7. The cycling performance of Li//CSE-3//S@C solid-state battery under 0.1 C at 60°C.

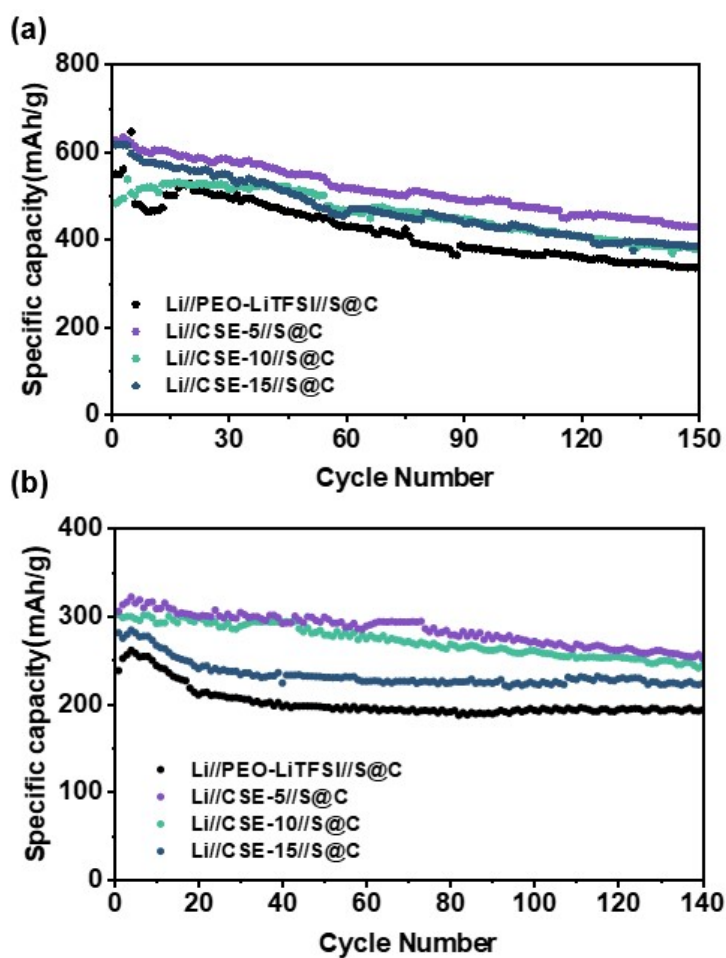


Figure S8. Cycling performance of Li//PEO-LiTFSI//S@C, Li//CSE-5//S@C, Li//CSE-10//S@C, and Li//CSE-15//S@C solid-state batteries at 40°C with the current density of (a) 0.05 C and (b) 0.1 C.

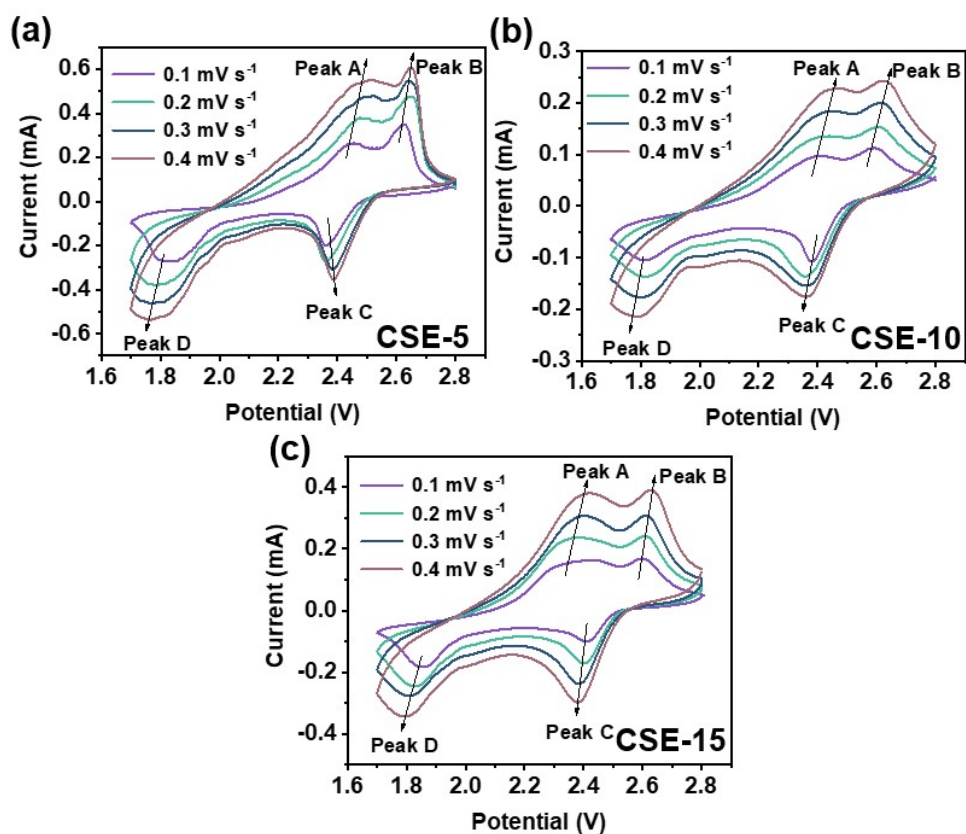


Figure S9. (a-c) CV curves of Li//CSE-5//S@C, Li//CSE-10//S@C, and Li//CSE-15//S@C solid-state batteries at different scan rates (0.1, 0.2, 0.3, and 0.4 mV s⁻¹) at 40°C.

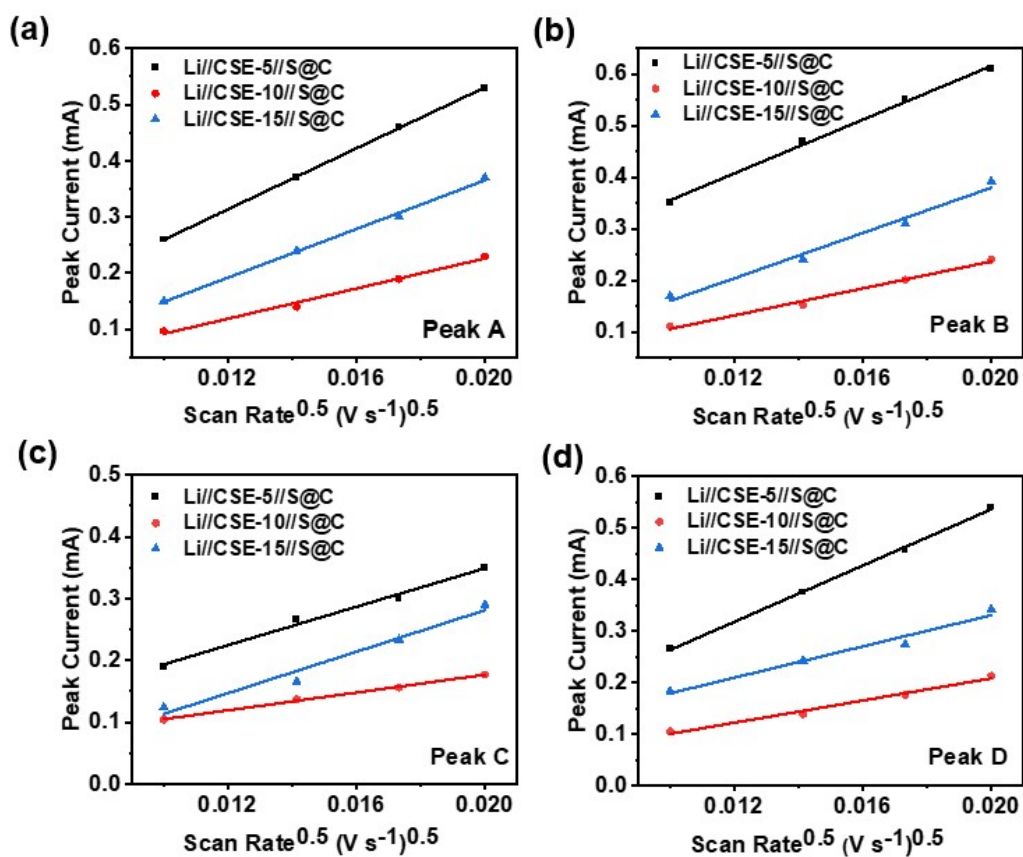


Figure S10. The peak current vs. scan rate linear plots of (a) oxidation peak A, (b) oxidation peak B, (c) reduction peak C, and (d) reduction peak D for Li//CSE-5//S@C, Li//CSE-10//S@C, Li//CSE-15//S@C solid-state batteries at 40°C.

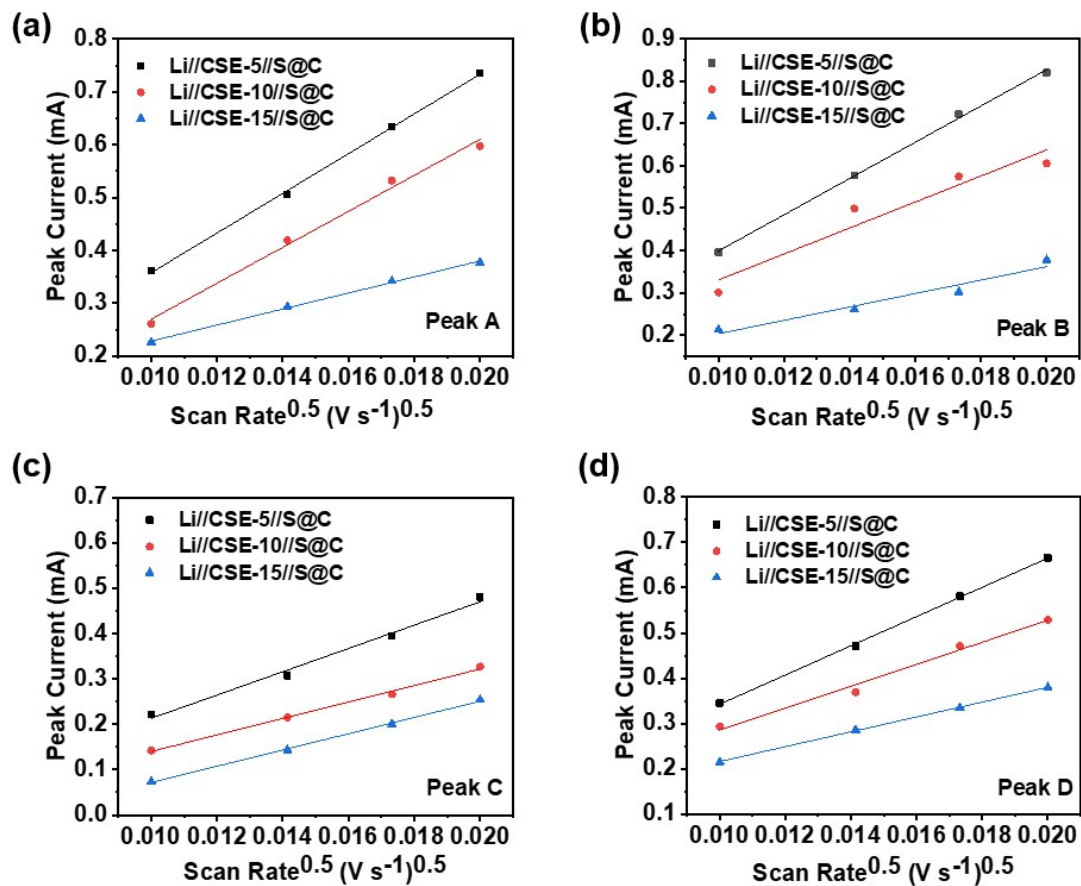


Figure S11. The peak current vs. scan rate linear plots of (a) oxidation peak A, (b) oxidation peak B, (c) reduction peak C, and (d) reduction peak D for Li//CSE-5//S@C, Li//CSE-10//S@C, and Li//CSE-15//S@C solid-state batteries at 60°C.

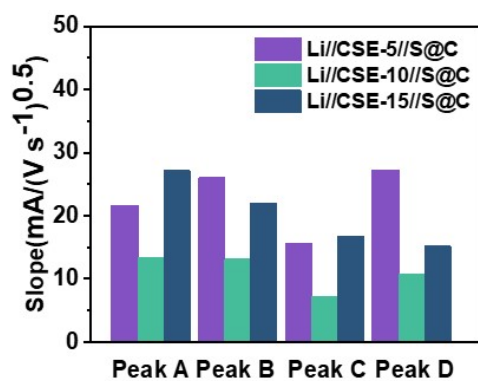


Figure S12. Slopes of fitted curves for different redox peaks at (a) 40°C in Li//CSE-5//S@C, Li//CSE-10//S@C, Li//CSE-15//S@C solid-state batteries.

